Biointerface Research in Applied Chemistry
Open-Access Journal (ISSN: 2069-5837)

Article
Volume 13, Issue 2, 2023, 115
https://doi.org/10.33263/BRIAC132.115

One-Step Synthesis of N/N-S Graphene from Fruitwastes: Chemistry and Mechanism

Jhuma Debbarma [1], Udayan Debnath [1], Mitali Saha [1,*]

[1] Department of Chemistry, National Institute of Technology Agartala, Tripura-799046, India
* Correspondence: mitalichem71@gmail.com (M.S.);

Scopus Author ID 5779373600
Received: 10.12.2021; Accepted: 6.12.2021; Published: 24.03.2022

Abstract: The present work explored the synthesis of N-S containing graphene from nitrogen-rich fruit wastes in the presence of urea and thiourea. Since pure graphene exhibited limited electrocatalytic activity due to a low number of active sites, it is highly recommended to introduce multi-heteroatoms into the graphitic lattice, increasing electrical conductivity and interlayer spacing graphene. The results suggested that urea and thiourea played a dual role as they were involved in the cyclization and aromatization to form a graphitic lattice and introduced nitrogen and sulfur atoms within the lattice pyrolysis. The utilization of urea and thiourea facilitated the development of N-S containing graphene from fruit wastes and prevented oxygen's attack between 250-350 ^{o}C under normal atmospheric conditions.

Keywords: Papaya seeds; watermelon rinds; banana peels; pyrolysis; N/N-S graphene; chemistry; mechanism.

1. Introduction

Many methods have been explored to prepare graphene derivatives for various applications [1-19]. However, it is now well known that both nitrogen and sulfur within graphitic lattice create more powerful active regions, resulting in better electrocapacitive and electrocatalytic activities than mono-doped graphene [20-38]. While nitrogen atoms can modulate the electronic properties of the carbon materials in the graphitic lattice, sulfur can easily polarize the electron pairs of carbon atoms, thereby enhancing the chemical reactivity of the doped carbon materials. Although several researchers reported the synthesis of N-S containing graphene, most of them require conventional graphite, dopants, corrosive oxidizers, high temperatures (>550 ^{o}C), etc. [39-42]. The present work explored the insertion of both nitrogen and sulfur during the in situ pyrolysis of nitrogen-rich fruit wastes in the presence of thiourea at relatively low temperatures.

In our previous works, emphasis was mainly given to ensure the selectivity of different carbon and nitrogen-rich fruit wastes towards the synthesis of nitrogen-containing graphene, bypassing the use of any additional N-dopants [43]. After the critical investigation of the chemistry and mechanism of nitrogen-containing fruit waste in developing N-graphene derivatives, it was planned to enhance the nitrogen contents within the graphitic lattice and develop N-S graphene for enhanced electrocatalytic efficiency. The role of easily available urea and thiourea in the formation of N-S graphene under normal atmospheric conditions was studied in detail, and interestingly, the results indicated the involvement of sulfur and diamine

structures of urea and thiourea in the cyclization and aromatization of the monomer molecules present in fruit wastes to form nanosheets of N-S graphene. This approach will offer more potential resources for producing N/N-S graphene from various waste materials, without graphite, harsh chemicals, and inert atmosphere, and stimulate competent applications in the biosensor, solar cell, water purification, energy storage, etc.

2. Materials and Methods

Papaya seeds, watermelon rinds, and banana peels were obtained from the local market. The resultant products obtained from all the precursors were characterized by X-ray diffraction (Bruker D8 advance diffractometer) in the 2θ range of 5 – 60º, FE-SEM (Sigma-300, Carl Zeiss) along with EDX and HRTEM (Jeol JEM-2100 microscope) at an acceleration voltage of 200 kV.

2.2. Preparation of N/N-S graphene from fruit wastes.

Three fruit wastes viz., papaya seeds, watermelon rinds, and banana peels were chosen to prepare N-Gr, washed thoroughly with deionized water, cut into small pieces, and dried for 72 hrs. These were further ground to give fine powders, separately mixed with urea at the ratio of 1:5 and heated to 250 ºC temperature. The black powders obtained after 2 hrs from all the precursors were washed with distilled water followed by 2 M nitric acid to remove the impurities. The resultant products were filtered and dried in the oven for 24 hrs. Similar to urea, the role of thiourea was also studied in the preparation of N-S graphene. Hence, the fine powders obtained after grinding the three fruit wastes were mixed with thiourea in a 1:5 ratio and subjected to pyrolysis at 250 ºC and 350 ºC. After 2 hrs, black powders formed in each case were washed, filtered, and dried in the oven for 24 hrs.

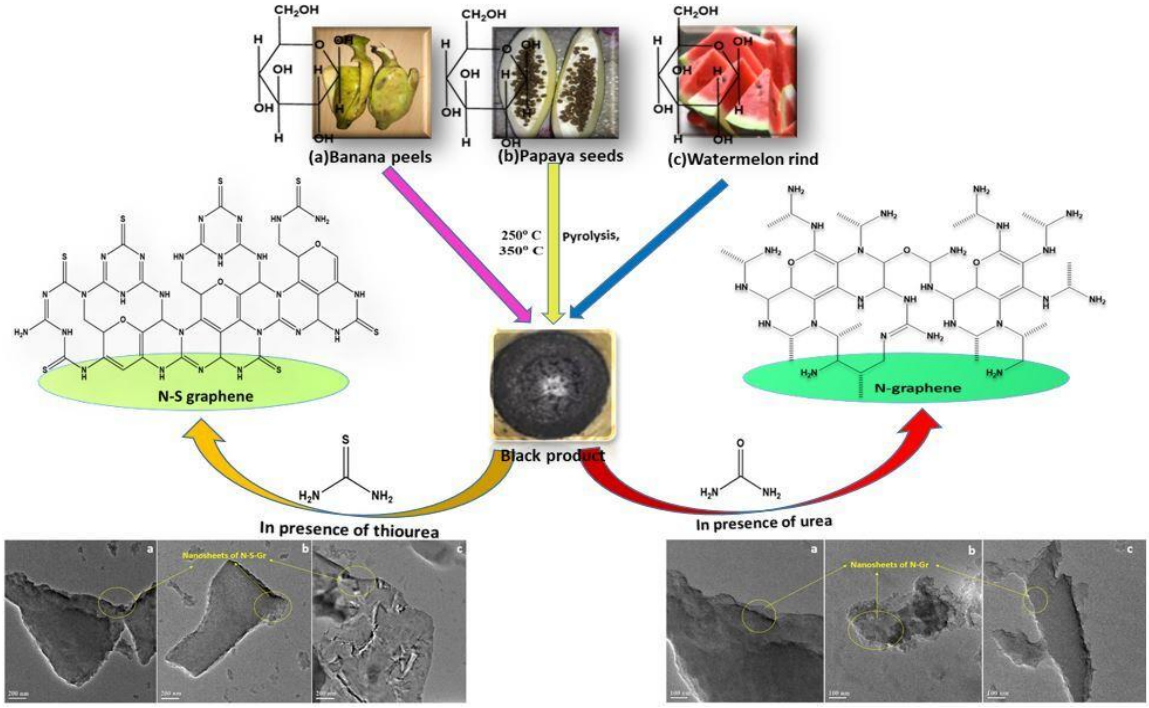

Scheme 1. Preparation of N/N-S graphene from nitrogen-rich fruit wastes in the presence of urea and thiourea at the temperature range of 250-350 ºC.

3. Results and Discussion

To study the involvement of diamine structures of urea in the one step formation of N-Gr, three fruit wastes viz. banana peels, papaya seeds, and watermelon rinds were subjected to pyrolysis at the temperature of 250 ºC, which resulted in the development of B-N-Gr, P-N-Gr, and W-N-Gr from all the three fruit wastes. The XRD patterns showed the peaks in the range 2θ of 26.5-26.9º at 250 ºC (Figure 1), indicating the direct conversion of fruit wastes to N-Gr in each case. Urea successfully prevented the functionalization of nitrogen-containing graphene by hindering the attack of oxygen.

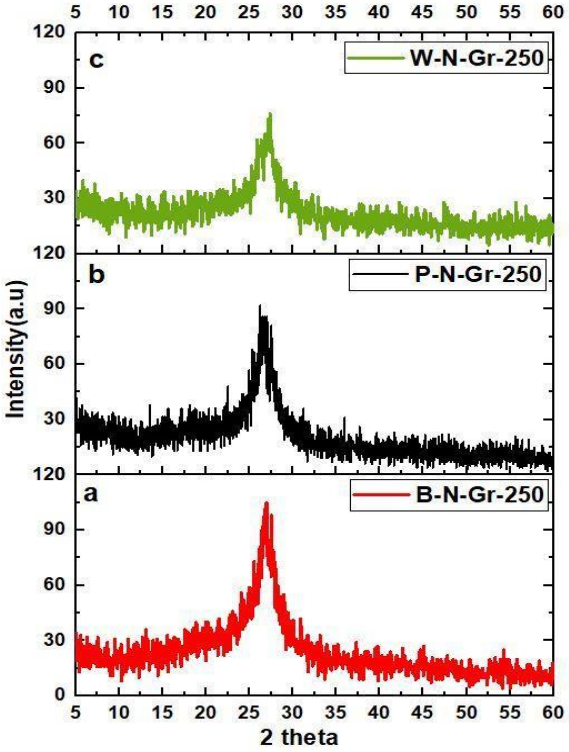

Figure 1. XRD patterns of (**a**) B-N-Gr; (**b**) P-N-Gr, and (**c**) W-N-Gr at 250 ºC.

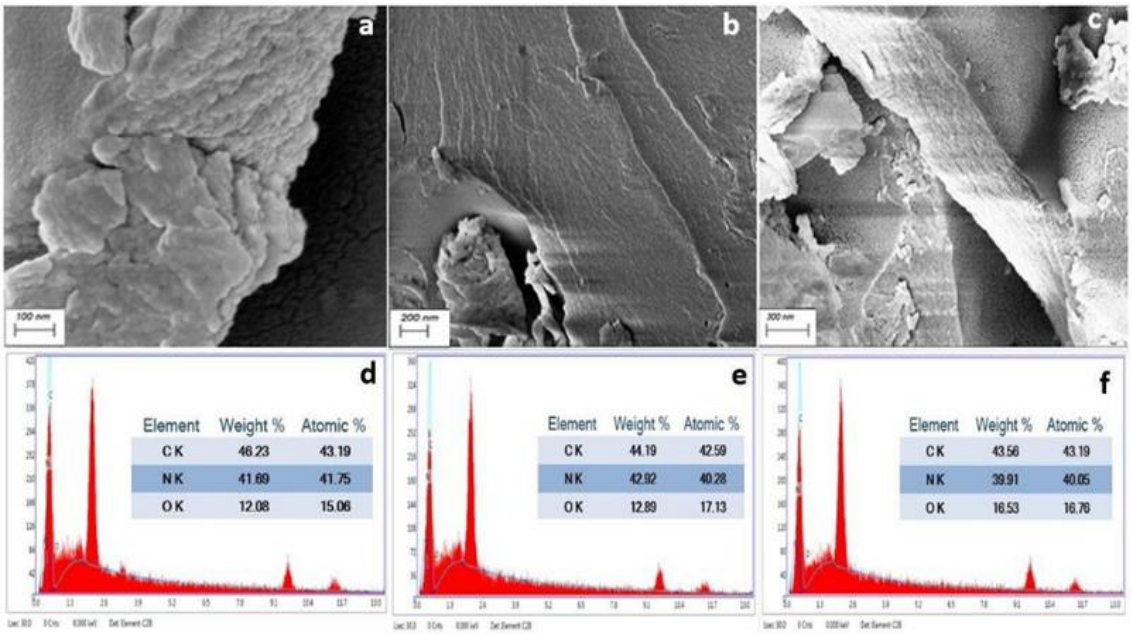

Figure 2. FESEM images of (**a**) B-N-Gr; (**b**) P-N-Gr and (**c**) W-N-Gr and EDX of (**d**) B-N-Gr, (**e**) P-N-Gr and (**f**) W-N-Gr at 250 ºC.

The FESEM images showed the formation of nanosheets of N-Gr (B-N-Gr, P-N-Gr, and W-N-Gr) in all the cases (Figure 2). The EDX analysis exhibited the carbon content from 43.5-46.2 %, whereas the nitrogen content was exceptionally high (40.0-42.9 %) in all the cases. The high amount of nitrogen in B-N-Gr, P-N-Gr, and W-N-Gr confirmed the involvement of the bent structure of urea in the cyclization and aromatization along with the monomer molecules present in fruit wastes. As a result, the heat treatment at 250 ^{o}C resulted in the direct conversion of fruit wastes to nitrogen-containing graphene in a single step. The presence of oxygen (~15%) indicated that the glucose molecules were intact within the graphitic lattice throughout the heat treatment. The TEM images showed the nanosheets in cases of B-N-Gr, P-N-Gr, and W-N-Gr (Figure 3 (a-c)).

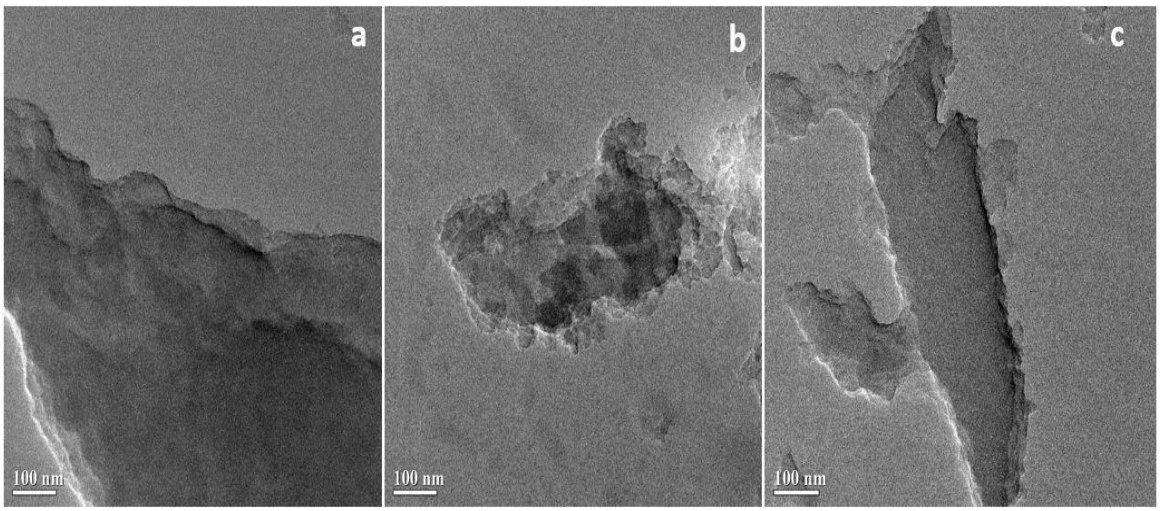

Figure 3. TEM images of **a**) B-N-Gr; (**b**) P-N-Gr, and (**c**) W-N-Gr at 250 ^{o}C.

The mechanism of formation of N-Gr has been presented in Figure 4, which indicated the formation of N-Gr from all the three fruit wastes as confirmed by the XRD pattern. In our earlier work, it was observed that these three nitrogen-rich fruit wastes played an important role in the progress of graphitic structure and formed nitrogen-containing graphene without using any additional nitrogen dopants [43]. Herein, the utilization of bent-structured urea was found to enhance the nitrogen content during cyclization with hydroxyl groups of monomer molecules, resulting in the dehydrogenation of existing polyaromatic rings of N-graphene.

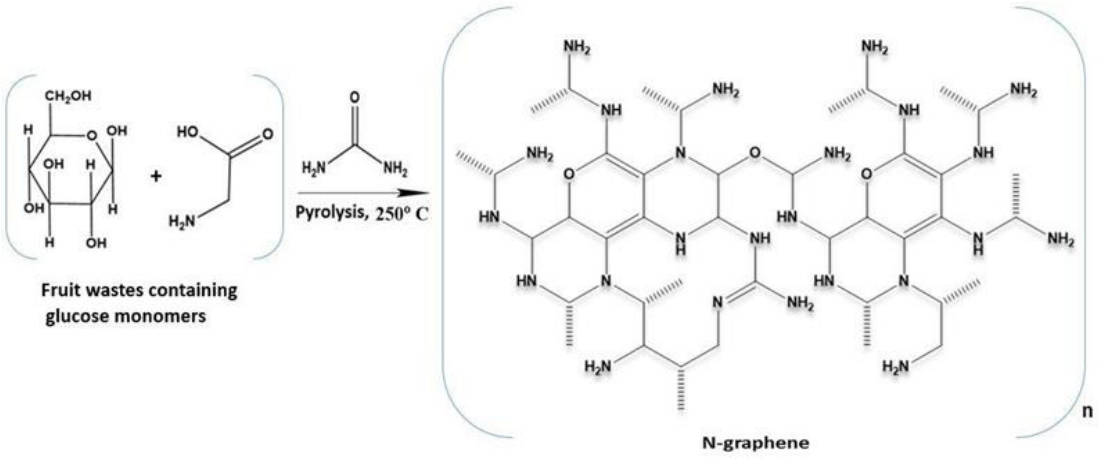

Figure 4. Mechanism of formation of N-Gr from papaya seeds, banana peels, and watermelon rinds at 250 ^{o}C.

Figure 5(a-c) showed the formation of graphene at 350 ^{o}C from the same precursors in the presence of thiourea. Due to the high melting temperature of thiourea (182 ^{o}C), it was not

able to convert the fruit wastes into N-S-Gr (B-N-S-Gr, P-N-S-Gr, and W-N-S-Gr) at 250 ºC. However, when the temperature was increased to 350 ºC, all the three fruit wastes were directly converted into nitrogen-sulfur-containing graphene in the presence of thiourea with an intense peak at 2θ of 26.8-27.1º (Figure 5(a-c)).

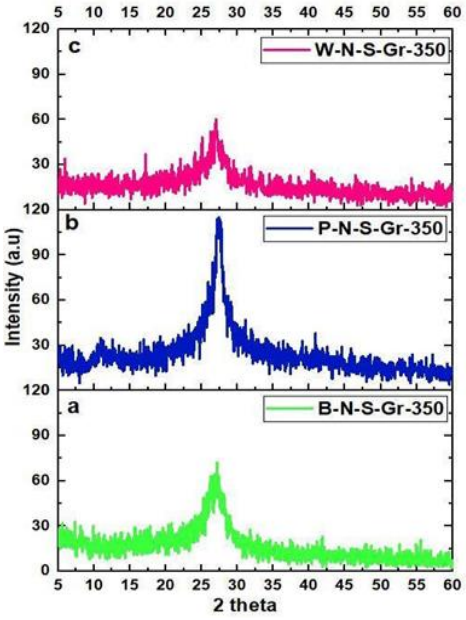

Figure 5. XRD patterns of (**a**) B-N-S-Gr; (**b**) P-N-S-Gr, and (**c**) W-N-S-Gr at 350 ºC.

The FESEM images showed the formation of nanosheets in all the fruit wastes (Figure 6(a-c)). The EDX showed the presence of 41.2-44 % of carbon, 38.2- 40 % of nitrogen, and 11.3-15.2 % of sulfur in the resulted products (Figure 6(d-f)). This also confirmed that the reducing nature of thiourea prevented the formation of functionalized graphene. The TEM images confirmed the formation of nanosheets for all three cases at 350 ºC (Figure 7(a-c)). Like urea, bent-structured thiourea also participated in the cyclization and aromatization of the monomeric glucose molecules present in fruit wastes, introducing nitrogen and sulfur within the graphitic lattice at 350 ºC (Figure 8).

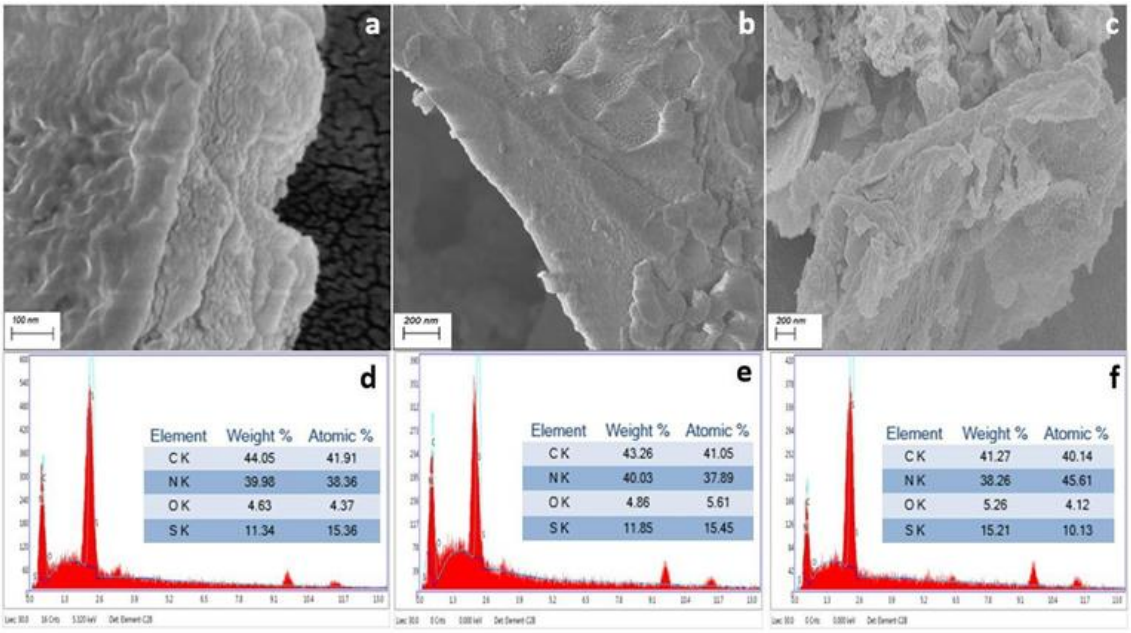

Figure 6. FESEM images of (**a**) B-N-S-Gr; (**b**) P-N-S-Gr and (**c**) W-N-S-Gr and EDX of (**d**) B-N-S-Gr; (**e**) P-N-S-Gr and (**f**) W-N-S-Gr at 350 ºC.

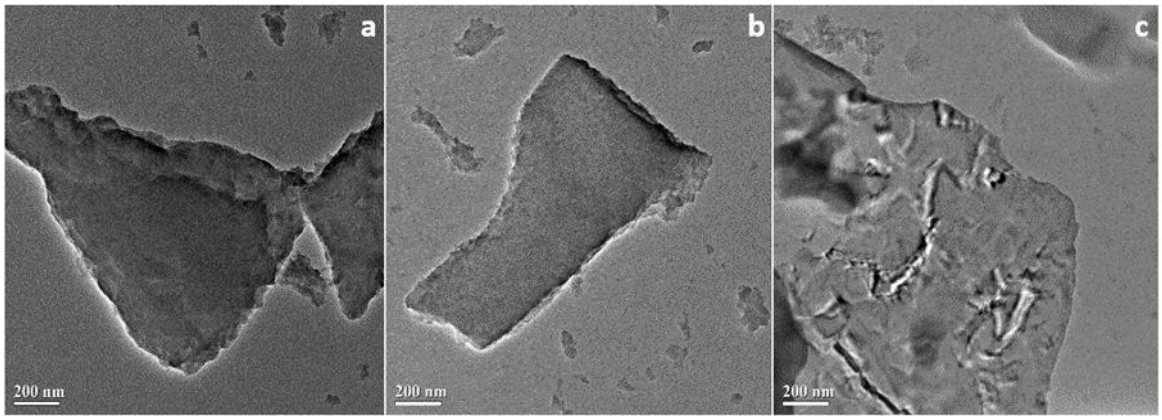

Figure 7. TEM images of (**a**) B-N-S-Gr; (**b**) P-N-S-Gr, and (**c**) W-N-S-Gr at 350 °C.

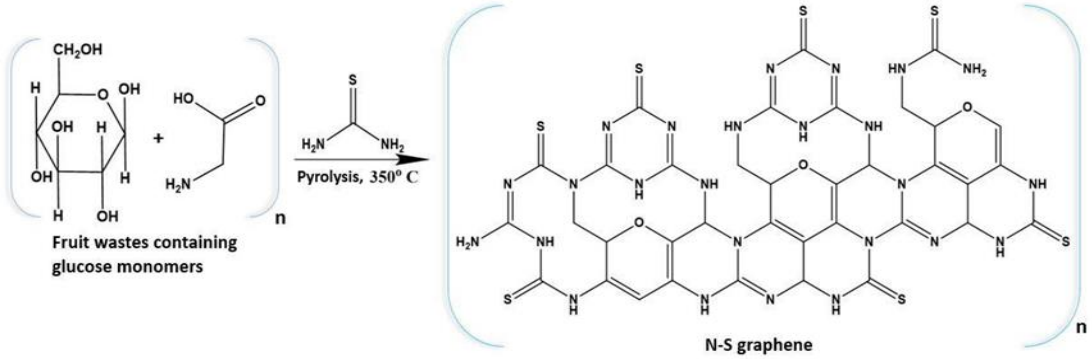

Figure 8. Mechanism of formation of N-S-Gr from papaya seeds, banana peels, and watermelon rinds at 350 °C.

4. Conclusions

One-step formation of N and N-S containing graphene from three fruit wastes was reported in the presence of urea and thiourea, which facilitated the direct conversion of precursors to N/N-S Gr at 250 and 350 °C, respectively. The results confirmed the participation of bent structures of both the urea and thiourea in the development of hexagonal ring systems of graphene. This approach can effectively synthesize multi heteroatoms containing graphene without the usage of toxic chemicals and an inert atmosphere. The proper utilization of waste materials for developing N/N-S graphene derivatives may prove to be cost-effective and eco-friendly. Hence, it can be the solution to fulfill the demand for graphene and its derivatives in various research fields.

Funding

This research received no external funding.

Acknowledgments

The authors like to thank the Central Research Facility of the National Institute of Technology Agartala for XRD data, Tripura University for SEM with EDX and North Eastern Hill University, Shillong for TEM micrographs.

Conflicts of Interest

The authors declare no conflict of interest.

References

1. Mohamad, A.; Rizwan, M.; Keasberry, N.A.; Ahmed, M.U. Fabrication of label-free electrochemical food biosensor for the sensitive detection of ovalbumin on nanocomposite-modified graphene electrode. *Biointerface Res. Appl. Chem.* **2019**, *9*, 4655-4662, https://doi.org/10.33263/briac96.655662.
2. Zindani, D.; Kumar, K. Graphene-based polymeric nano-composites: an introspection into functionalization, processing techniques and biomedical applications. *Biointerface Res. Appl. Chem.* **2019**, *9*, 3926-3933, https://doi.org/10.33263/briac93.926933.
3. Elazab, H.A.; Gadalla, M.A.; Sadek, M.A.; El-Idreesy, T.T. Hydrothermal synthesis of graphene supported Pd/Fe3O4 nanoparticles as efficient magnetic catalysts for Suzuki Cross - Coupling. *Biointerface Res. Appl. Chem.* **2019**, *9*, 3906-3911, https://doi.org/10.33263/briac92.906911.
4. Pham, T.T.; Monajjemi, M.; Dang, D.M.T.; Mollaamin, F.; Dang, C.M. Nano-capacitors as batteries including graphene electrodes and Ga-N mixed with biopolymers as insulator. *Biointerface Res. Appl. Chem.* **2019**, *9*, 3806-3811, https://doi.org/10.33263/briac91.806811.
5. Faisal, N. Mechanical Behavior of Nano-Scaled Graphene Oxide Reinforced High-Density Polymer Ethylene for Orthopedic Implants. *Biointerface Res. Appl. Chem.* **2020**, *10*, 7223-7233, https://doi.org/10.33263/briac106.72237233.
6. Daoudi, K.; Gaidi, M.; Columbus, S. Silver nanoprisms/graphene oxide/silicon nanowires composites for R6G surface-enhanced Raman spectroscopy sensor. *Biointerface Res. Appl. Chem.* **2020**, *10*, 5670-5674, https://doi.org/10.33263/briac103.670674.
7. Swamy, B.K.; Shiprath, K.; Rakesh, G.; Ratnam, K.V.; Manjunatha, H.; Janardan, S.; Naidu, K.C.B.; Ramesh, S.; Suresh, K.; Ratnamala, A. Simultaneous detection of dopamine, tyrosine and ascorbic acid using NiO/graphene modified graphite electrode. *Biointerface Res. Appl. Chem.* **2020**, *10*, 5599-5609, https://doi.org/10.33263/briac103.599609.
8. Prabakar, A.C.; Killivalavan, G.; Sivakumar, D.; Naidu, K.C.B.; Sathyaseelan, B.; Senthilnathan, K.; Baskaran, I.; Manikandan, E.; Rao, B.R.; Sarma, M., et al. Structural, morphological, and magnetic properties of copper zinc cobalt ferrites systems nanocomposites. *Biointerface Res. Appl. Chem.* **2020**, *10*, 6015-6019, https://doi.org/10.33263/briac104.015019.
9. Sun, X.L.; Qi, Z.; Li, Q.Q.; Zhang, X.R.; Shao, X.L.; Jin, Y.; Zhang, J.J.; Liu, Y.Y. Utilization of carbon nanotube and graphene in electrochemical CO2 reduction. *Biointerface Res. Appl. Chem.* **2020**, *10*, 5815-5827, https://doi.org/10.33263/briac104.815827.
10. Olabi, A. G.; Abdelkareem, M. A.; Wilberforce, T.; Sayed, E. T. Application of graphene in energy storage device–A review. *Renew. Sust. Energ. Rev.* **2021**, *135*, 110026, https://doi.org/10.1016/j.rser.2020.110026.
11. Hu, Y.; Zhou, C.; Wang, H.; Chen, M.; Zeng, G.; Liu, Z.; Liang, Q. Recent advance of graphene/semiconductor composite nanocatalysts: Synthesis, mechanism, applications and perspectives. *Chem. Eng. J.* **2021**, *414*, 128795, https://doi.org/10.1016/j.cej.2021.128795.
12. Li, Z.; Lei, H.; Kan, A.; Xie, H.; Yu, W. Photothermal applications based on graphene and its derivatives: a state-of-the-art review. *Energy*, **2021**, *216*, 119262, https://doi.org/10.1016/j.energy.2020.119262.
13. Ponnamma, D.; Yin, Y.; Salim, N.; Parameswaranpillai, J.; Thomas, S.; Hameed, N. Recent progress and multifunctional applications of 3D printed graphene nanocomposites. *Compos. B. Eng.* **2021**, *204*, 108493, https://doi.org/10.1016/j.compositesb.2020.108493.
14. Bashir, B.; Khalid, M. U.; Aadil, M.; Zulfiqar, S.; Warsi, M. F.; Agboola, P. O.; Shakir, I. CuxNi1-xO nanostructures and their nanocomposites with reduced graphene oxide: synthesis, characterization, and photocatalytic applications. *Ceram. Int.* **2021**, *47*, 3603-3613, https://doi.org/10.1016/j.ceramint.2020.09.209.
15. Mandal, P.; Debbarma, J.; Saha, M. A Review on the Emergence of Graphene in Photovoltaics Industry. *Biointerface Res. Appl. Chem.* **2021**, *11*, 15009-15036, https://doi.org/10.33263/BRIAC116.1500915036.
16. Lingamdinne, L. P.; Lee, S.; Choi, J. S.; Lebaka, V. R.; Durbaka, V. R. P.; Koduru, J. R. Potential of the magnetic hollow sphere nanocomposite (graphene oxide-gadolinium oxide) for arsenic removal from real field water and antimicrobial applications. *J. Hazard. Mater.* **2021**, *402*, 123882, https://doi.org/10.1016/j.jhazmat.2020.123882.
17. Brzhezinskaya, M.; Kononenko, O.; Matveev, V.; Zotov, A.; Khodos, I. I.; Levashov, V.; Roshchupkin, D. Engineering of Numerous Moiré Superlattices in Twisted Multilayer Graphene for Twistronics and Straintronics Applications. *ACS nano.* **2021**, *15*, 12358-12366, https://doi.org/10.1021/acsnano.1c04286.
18. Su, H.; Hu, Y. H. Recent advances in graphene-based materials for fuel cell applications. *Energy Sci. Eng.* **2021**, *9*, 958-983, https://doi.org/10.1002/ese3.833.
19. Ayub, S.; Guan, B. H.; Ahmad, F.; Oluwatobi, Y. A.; Nisa, Z. U.; Javed, M. F.; Mosavi, A. Graphene and Iron Reinforced Polymer Composite Electromagnetic Shielding Applications: A Review. *Polymers* **2021**, *13*, 2580, https://doi.org/10.3390/polym13152580.

20. Shanmugam, R.; Manavalan, S.; Chen, S. M.; Keerthi, M.; Lin, L. H. Methyl Parathion Detection Using SnS2/N, S–Co-Doped Reduced Graphene Oxide Nanocomposite. *ACS Sustain. Chem. Eng.* **2020**, *8*, 11194-11203, https://doi.org/10.1021/acssuschemeng.0c02528.
21. Zhu, J.; Tu, W.; Pan, H.; Zhang, H.; Liu, B.; Cheng, Y.; Zhang, H. Self-templating synthesis of hollow Co3O4 nanoparticles embedded in N, S-dual-doped reduced graphene oxide for lithium-ion batteries. *ACS nano*, **2020**, *14*, 5780-5787, https://doi.org/10.1021/acsnano.0c00712.
22. Cheng, S.; Duan, X.; Zhang, Z.; An, D.; Zhao, G.; Liu, Y. Preparation of a natural rubber with high thermal conductivity, low heat generation and strong interfacial interaction by using NS-modified graphene oxide. *Mater. Sci.* **2021**, *56*, 4034-4050, https://doi.org/10.1007/s10853-020-05503-8.
23. Wu, D.; Wang, T.; Wang, L.; Jia, D. Hydrothermal synthesis of nitrogen, sulfur co-doped graphene and its high performance in supercapacitor and oxygen reduction reaction. *Microporous Mesoporous Mater.* **2019**, *290*, 109556, https://doi.org/10.1016/j.micromeso.2019.06.018.
24. Kumar, R.; Macedo Jr, W. C.; Singh, R. K.; Tiwari, V. S.; Constantino, C. J.; Matsuda, A.; Moshkalev, S. A. Nitrogen–sulfur co-doped reduced graphene oxide-nickel oxide nanoparticle composites for electromagnetic interference shielding. *ACS Appl. Nano Mater.* **2019,** *2*, 4626-4636, https://doi.org/10.1021/acsanm.9b01002.
25. Han, W.; Chen, L.; Song, W.; Wang, S.; Fan, X.; Li, Y.; Peng, W. Synthesis of nitrogen and sulfur co-doped reduced graphene oxide as efficient metal-free cocatalyst for the photo-activity enhancement of CdS. *Appl. Catal. B.* **2018**, *236*, 212-221, https://doi.org/10.1016/j.apcatb.2018.05.021.
26. Wang, J.; Yang, Y.; Jia, L.; Yang, N.; Guan, Q.; Huang, L.; Ning, P. The influence of the charge compensating anions of layered double hydroxides (LDHs) in LDH-NS/graphene oxide nanohybrid for CO2 capture. *J. Nanosci. Nanotechnol.* **2018**, *18*, 2956-2964, https://doi.org/10.1166/jnn.2018.14381.
27. Zhang, Z.; Liu, X.; Yu, C.; Zhou, W.; Li, F. One-step hydrothermal synthesis of NS-GQDs/Bi2S3 microrods with highly photocatalytic performance for Cr (VI) reduction. *Colloids Surf. A Physicochem. Eng.* **2021**, *626*, 127109, https://doi.org/10.1016/j.colsurfa.2021.127109.
28. Chen, Y.; Liu, Z.; Sun, L.; Lu, Z.; Zhuo, K. Nitrogen and sulfur co-doped porous graphene aerogel as an efficient electrode material for high performance supercapacitor in ionic liquid electrolyte. *J. Power Sources.* **2018**, *390*, 215-223, https://doi.org/10.1016/j.jpowsour.2018.04.057.
29. Mannan, A.; Hirano, Y.; Quitain, A. T.; Koinuma, M.; Kida, T. Nitrogen, Sulfur Co-Doped Reduced Graphene Oxide: Synthesis and Characterization. *Micro Nanosyst.* **2020**, *12*, 129-134, https://doi.org/10.2174/1876402911666190722111138.
30. Li, Q.; Bai, A.; Xue, Z.; Zheng, Y.; Sun, H. Nitrogen and sulfur co-doped graphene composite electrode with high electrocatalytic activity for vanadium redox flow battery application. *Electrochim Acta.* **2020**, *362*, 137223, https://doi.org/10.1016/j.electacta.2020.137223.
31. Hasan, M. T.; Gonzalez-Rodriguez, R.; Ryan, C.; Faerber, N.; Coffer, J. L.; Naumov, A. V. Photo-and Electroluminescence from Nitrogen-Doped and Nitrogen–Sulfur Codoped Graphene Quantum Dots. *Adv. Funct. Mater.* **2018**, *28*, 1804337, https://doi.org/10.1002/adfm.201804337.
32. Zhang, K.; Chen, X.; Li, Z.; Wang, Y.; Sun, S.; Guo, T.; Lu, X. Au-Pt bimetallic nanoparticles decorated on sulfonated nitrogen sulfur co-doped graphene for simultaneous determination of dopamine and uric acid. *Talanta*, **2018**, *178*, 315-323, https://doi.org/10.1016/j.talanta.2017.09.047.
33. Zhang, R.; Zhang, C.; Zheng, F.; Li, X.; Sun, C. L.; Chen, W. Nitrogen and sulfur co-doped graphene nanoribbons: a novel metal-free catalyst for high performance electrochemical detection of 2, 4, 6-trinitrotoluene (TNT). *Carbon*, **2018**, *126*, 328-337, https://doi.org/10.1016/j.carbon.2017.10.042.
34. Kumar, R.; Sahoo, S.; Joanni, E.; Singh, R. K.; Maegawa, K.; Tan, W. K.; Matsuda, A. Heteroatom doped graphene engineering for energy storage and conversion. *Mater. Today.* **2020**, *39*, 47-65, https://doi.org/10.1016/j.mattod.2020.04.010.
35. Shi, J.; Wang, Y.; Su, Q.; Cheng, F.; Kong, X.; Lin, J.; Pan, A. NS co-doped C@ SnS nanoflakes/graphene composite as advanced anode for sodium-ion batteries. *Chem. Eng. Technol.* **2018**, *353*, 606-614, https://doi.org/10.1016/j.cej.2018.07.157.
36. Domga; Karnan, M.; Oladoyinbo, F.; Noumi, G. B.; Tchatchueng, J. B.; Sieliechi, M. J.; Sathish, M.; Pattanayak, D. K. A simple, economical one-pot microwave assisted synthesis of nitrogen and sulfur co-doped graphene for high energy supercapacitors. *Electrochim Acta* **2020**, *341*, 135999, https://doi.org/10.1016/j.electacta.2020.135999.
37. Sajjadi, S.; Khataee, A.; Soltani, R. D. C.; Hasanzadeh, A. N, S co-doped graphene quantum dot–decorated Fe3O4 nanostructures: Preparation, characterization and catalytic activity. *J Phys Chem Solids.* **2019**, *127*, 140-150, https://doi.org/10.1016/j.jpcs.2018.12.014.
38. Ruan, J.; Yuan, T.; Pang, Y.; Luo, S.; Peng, C.; Yang, J.; Zheng, S. Nitrogen and sulfur dual-doped carbon films as flexible free-standing anodes for Li-ion and Na-ion batteries. *Carbon* **2018**, *126*, 9-16, https://doi.org/10.1016/j.carbon.2017.09.099.

39. Zhou, G.; Paek, E.; Hwang, G. S.; Manthiram, A. Long-life Li/polysulphide batteries with high sulphur loading enabled by lightweight three-dimensional nitrogen/sulphur-codoped graphene sponge. *Nat. Commun.* **2015**, *6*, 1-11, https://doi.org/10.1038/ncomms8760.
40. Yu, X.; Zhang, M.; Chen, J.; Li, Y.; Shi, G. Nitrogen and sulfur codoped graphite foam as a self-supported metal-free electrocatalytic electrode for water oxidation. *Adv. Energy Mater.* **2016**, *6*, 1501492, https://doi.org/10.1002/aenm.201501492.
41. Wang, X.; Wang, J.; Wang, D.; Dou, S.; Ma, Z.; Wu, J.; Wang, S. One-pot synthesis of nitrogen and sulfur co-doped graphene as efficient metal-free electrocatalysts for the oxygen reduction reaction. *Chem. Commun.* **2014**, *50*, 4839-4842, https://doi.org/10.1039/c4cc00440j.
42. Kumari, S.; Verma, E.; Kumar, R.; Upreti, D.; Prakash, B.; Maruyama, T.; Bagchi, V. Micropores within N, S co-doped mesoporous 3D graphene-aerogel enhance the supercapacitive performance. *New J. Chem.* **202**1, *45*, 7523-7532, https://doi.org/10.1039/D1NJ00459J.
43. Debbarma, J.; Mandal, P.; Saha, M. Fruit wastes to N-containing graphene: chemistry and mechanism. *Fuller Nanotub Car N.* **2021**, *29*, 1-7, https://doi.org/10.1080/1536383X.2021.1889517.